

Effect of Process Parameters on the Properties of Clay-Based Composite Filter for Water Purification

A. D. Adeyinka-Aderanti^{1*}, A. A. Agbelele², F.O. Agunbiade³, J.O. Agunsoye⁴

^{1,2,4}Department of Metallurgical and Materials Engineering, University of Lagos, Nigeria

³Department of Chemistry, University of Lagos, Nigeria

Email: adedayoaderanti23@gmail.com

Abstract

Consumption of contaminated water causes disease infections which are highly contagious and can lead to loss of lives and reduction in life expectancy. More than half of Africans live in rural areas and these people have a larger share of an inadequate supply of safe drinking water. This study is aimed at producing a clay composite filter that will effectively remove contaminants from water and provide safe drinking water for rural dwellers. The materials, temperature and characterization stage of the filter production were considered. Activated carbon produced by carbonization of coconut shell and activation using lime juice and water was blended with micron size clay and coconut shell nano particle. The blend contains clay, activated carbon and coconut shell nanoparticle in the ratio 60: 30: 10, 60: 20: 20, 60: 10: 30, and 60: 0: 40, and then sintered at temperature of 700 °C, 800 °C, 900 °C, and 1000 °C. The surface area and pore size of the blends after firing were tested using Brunauer-Emmett-Teller (BET). The microstructure and crystal structure were examined and determined using Scanning Electron Microscopy/Energy Dispersive Spectroscopy (SEM/EDS) and X-ray Diffractometer (XRD) respectively. The results showed that the mix of 60: 10: 30, fired at 900 °C gave the best parameters for the production of clay filter with better flow rate, pore size, and pore volume measurements.

Keywords: Activated carbon, clay hybrid filter, coconut shell nanoparticle, water contamination, water purification

1.0 INTRODUCTION

According to the United Nations Sustainable Development Goal 6 target 6.1 from 2016 to 2030 regarding access to safe water and sanitation, it is expected that by 2030, there should be universal and affordable access to safe water for all (United Nations, 2023). Only 74 % of the world's population has access to quality supply of drinking water in 2020 which indicates a 4 % increase since the SDG was set in 2016 (WHO/UNICEF, 2021). At this rate, only 81% of the world population will have access to safe and affordable drinking water sources by 2030 as opposed to the proposed >99 % except there is a four times increase in the current progress rate. Therefore, the efforts of researchers, government agencies, NGOs, and relevant stake holders are needed four times more than before if safe water is to be made available for all in the next 7 years (by 2030). It should be noted that eight out of every ten people lacking supply of basic drinking water lived in rural areas and sub-saharan Africa and has 70 % of its population still in need of a safe drinking water supply (WHO/UNICEF, 2021). In lieu of this, research around water treatment and purification is required, particularly in rural areas of developing countries like Nigeria having more than 63 % of its population residing in rural areas and only 4 % has access to safe and affordable drinking water supply (Erhuanga *et al*, 2021; NBS and UNICEF, 2017).

Nigeria is among the countries in which only about 25% of the population has access to safely managed drinking water and this is the case with most African countries. Invariably, out of the over 200 million Nigerians, less than 50 million have a safe water source. Most Nigerians depend on surface and ground water sources for drinking water and these sources are prone to contaminations from both natural and manmade activities which in turn lead to the spread of various water borne diseases in the country. The safety of water for drinking is linked to the sanitation level of the environment. Now, only 54 % of the world's population uses safely

managed sanitation leaving more than 2.8 billion people with no safe sanitation method and almost 500 million people still practice open defecation (WHO/UNICEF, 2021). An estimate of about 46 million people in Nigeria practice open defecation which aided the development of an initiative by the Federal Ministry of Water Resources (supported by UNICEF) to make Nigeria free of open defecation by 2025 (UNICEF, 2023). The initiative aims at providing adequate water supply and sanitation services for rural dwellers. However, this aim is yet to be achieved as most people in rural areas still lack proper sanitation and water supply. This indicates that although adequate sanitation is a long-lasting means of preventing water contamination, Nigeria is nowhere near achieving adequate sanitation for all and water is still being contaminated.

Nigeria and other sub-Saharan African countries have low levels of sanitation, and safe drinking water support leading to high reports of water-related illness (Babangida, Aslanova and Elkiran, 2022). Water related illnesses like cholera, diarrhea, typhoid, dysentery is one of the leading causes of diseases worldwide. Eight-hundred and forty-two thousand (842,000) people are estimated to die each year from diarrhea and about 240 million people are affected by an acute and chronic disease caused by parasitic worms in water called schistosomiasis (WHO, 2021) causing a reduction in people's life expectancy. Although there is paucity of information on cases of water related diseases in Nigeria, it is important to note that these diseases can lead to death and reduction of life expectancy of the bulk of the population in rural areas.

Point-of-use (POU) filtration system is a favorable solution to the provision of safe drinking water to rural dwellers (WHO/UNICEF, 2014). The idea behind POU filtration system is to remove the possibility of contamination in-transit. Composite clay-based water filter (CCWF) is an example of POU filtration system (Murphy *et al.*, 2010a, b; Kallman *et al.*, 2011; Mellor *et al.*, 2014; Berg, 2015; Farrow *et al.*, 2018) and it is the focal point of this paper. Other POU water treatment technologies are ultraviolet irradiation/ solar disinfection, bio-sand filtration, membrane filtration, ion exchange, biological filtration, chlorination, and candle filters among others (National Research Council, 1999; Murphy *et al.*, 2010c; Pagsuyoin *et al.*, 2015; Perez-Vidal *et al.*, 2016; Santos *et al.*, 2016), most of which are gradually dating out except for chlorination and candle filters. In this study, filter samples were produced using locally sourced materials (clay and coconut shell). The coconut shell was activated so that the filter sample was made out of different blends clay, coconut shell and activated carbon. The idea behind adding activated carbon to the blend is so that the filter can adsorb chemical substances that might be present in water. Also, the coconut shell used in this study was in nano particle scale so that the pores in the final filter samples will be small enough to trap other physical and biological contaminants in water.

2.0 MATERIALS AND METHODS

In the production of clay-based filter, the basic method involves sintering at elevated temperature with different blends of clay and carbonaceous material. In this study, the material blends include clay, coconut shell and activated carbon mixed at different proportions and sintered at temperatures ranging from 700 °C to 1000 °C. The method adopted in this study is a slight deviation from the commonly used micron sized, with the adoption of Nano particle size and addition of activated carbon to the blend for making clay composite filters.

2.1 Materials

Materials used for this study are clay and coconut shell. The clay was collected from Clay company, Oregun. Coconut shell was sourced from retail coconut sellers in an open market and

waste dump. Lemon was used for activation of coconut shell carbon. The filter material is a combination of clay, coconut shell, and coconut shell based activated carbon (Figure 1 a to c).

2.2 Materials preparation

2.2.1 Drying of Clay and Coconut Shell

The clay was dried in the oven (DHG – 9030, S.N 42225) at a temperature of 100 °C for 4 hours. The coconut shell was washed and oven dried at a temperature of 110 °C for 5 hours. The activated carbon was oven dried at 110 °C for 5 hours. The activated carbon was left to cool in the oven. The drying process for all these materials was carried out to remove any moisture present in the materials.



Figure 1(a): As sourced Clay



Figure 1(b): Coconut shell



Figure 1(c): Lemon

2.2.2 Crushing and Grinding of Coconut Shells and Clay

The coconut shell obtained after drying was crushed with hammer to smaller sizes (Figure 2a), then grinded to particle size (Figure 2b) using a pulverizer (RPMP/01 Model) operated at 3500 r.p.m. and 1.5 h.p. The clay was also grinded using a pulverizer (Figure 2c).



Figure 2(a): Crushed coconut shell



Figure 2(b): Pulverized coconut shell



Figure 2(c): Pulverized clay

2.2.3 Milling of Coconut Shell

Some of the pulverized coconut shell was milled using a planetary ball mill (JC – QM – 2; JC2021 - 072367). The pulverized coconut shell was measured in to the different compartment of the ball mill for material placement. The machine was operated at 280 r.p.m. This was done to achieve a nanoparticle sized CS. The milling lasted for about 16 hours and **Transmission Electron Microscopy (TEM)** was done to ascertain the attainment of nanoparticle size with samples taken at 8 hours and 16 hours of milling. The physical indication that the CS are in Nano-size range is the seeming start of agglomeration to the container.

2.2.4 Carbonization

The pulverized coconut shell was carbonized at 800 °C, for 4 hours (Saputro *et al*, 2020). Carbonization was carried out in a heat treatment furnace (SXL – 1208; 1905741) with

temperature control range of 400 ° - 1200 °C. The pulverized coconut shell was first poured into a fabricated steel box lined with refractory material to prevent oxidation. SEM/EDS analysis was used to ascertain that the coconut shell is carbonized. The carbonized coconut shell is shown in Figure 4a. The carbonization temperature of 800 °C was achieved at a heating rate of 200 °C/hr, then it was held in the furnace for 4 hours before being allowed to cool in the furnace.

2.2.5 Coconut Shell Activation Process

The carbonized coconut shell (CCS) was then activated through a local activation process using lemon and water mixture. 500 ml of freshly squeezed lemon juice was mixed with 1500 mL of water (1 lemon juice: 3 water) (Figure 3b). The CCS was poured gradually into the mixture until a paste-like texture is gotten (Figure 3c). 1000 g of CCS was mixed with the liquid mixture. The mixture was left in an airtight bucket for 24 hours. The mixture of lime water and CCS was then rinsed with water to remove the smell before being transferred to a flat plate for the water to flow out and then oven dried at 110 °C for 5 hours. Brunauer-Emmett-Teller (BET) test was used to measure the surface area of the activated carbon produced, to check if it is in line with the necessary measurements for activated carbon and Scanning Electron Microscopy/Energy Dispersive Spectroscopy (SEM/EDS) was carried out on the CCS and activated carbon to visualize the increase in carbon because of activation.



Figure 3(a): Lemon juice



Figure 3 (b): Lemon juice + water



Figure 3 (c): Mixture

2.2.6 Sieving of Clay and Activated Carbon

The pulverized clay was sieved with an electric power shaker using sieves of size 75, 150, 212, 300, 425, 600 and 1.18 microns respectively (200, 100, 72, 52, 36, 25, and 14 BSS). The clay in 75 and less than 75 μm sieve was used for the filter blend because it gave the highest yield (about 200 g in 500 g charge). The activated carbon in the 300-micron sieve was also used for the filter blend with yield of 282 g per 500 g charge.

2.3 Production of Sample Filters

2.3.1 Mixing

The clay, coconut shell nanoparticle (CSNP), and AC were mixed using sieve before being transferred to the electric mixture to obtain homogenous mixture. Then in a ball mill for 30 minutes. The Clay, activated carbon, and coconut shell nanoparticle blend were mixed in four different blends; 60:30:10, 60:20:20, 6:10:30, and 60:0:40 wt.%. A mix of 600 g of 60:30:10 contained 360 g of Clay, 180 g Activated carbon and 60 g of coconut shell nanoparticle. Water that was added to the blends is 10% of the total composition in g. The mixed blends were set aside in air tight containers.

2.3.2 Compaction

The mixed blends were then mixed with water. For a mixture of 600 g, 60 mL of water was added, which is 10% of the mix. The mixed blend was measured to 50 g for the formation of the samples. The weighed 50 g mix was poured into a rammer and set to ram, then removed. The compacted samples is as shown in Figure 4. The rammed samples have diameter of 5.0 cm and height of about 1.6 cm.



Figure 4: Compacted filter samples

2.3.3 Sintering of Compacted Filter Samples

The sintering of blends was carried out using a heat treatment furnace at temperatures 700 °C, 750 °C, 800 °C, 850 °C, 900 °C, 950 °C, and 1000 °C respectively (Figure 5, Table 1). The samples with different blends of composition will be sintered at different temperatures. The sintering process should cause burning out of carbonaceous material in the blend (that is NPCS) leaving pores in the samples. After firing the sample diameter became 4.8 cm and height was 1.5 cm



Figure 5: Fired filter samples

Table 1: Composition of Clay composite filter samples produced

		Temperature (°C)						
		1000	950	900	850	800	750	700
Composition	1	2	3	4	5	6	7	
	A	60Cl:30AC:10 CSNP	60:30:10	60:30:10	60:30:10	60:30:10	60:30:10	60:30:10
	B	60Cl:20AC:20 CSNP	60:20:20	60:20:20	60:20:20	60:20:20	60:20:20	60:20:20
	C	60Cl:10AC:30 CSNP	60:10:30	60:10:30	60:10:30	60:10:30	60:10:30	60:10:30
	D	60Cl:0AC:40 CSNP	60:0:40	60:0:40	60:0:40	60:0:40	60:0:40	60:0:40

Where AC is Activated Carbon and CSNP is Coconut shell Nanoparticle

2.4 Characterization of Raw materials and Filter Samples

The equipment used for characterization were:

X-Ray Diffractometer (XRD): Clay and sample filters were analysed using a PAnalytical X-Ray Diffractometer with X'Pert High score software. The operating temperature was 25 °C and the operation was conducted in a step size of 2Theta°.

X-ray fluorescence: Malvern PANalytical XRF spectrometer with software version 10.3.0.159 was used at 20kV and 25 mA to determine the elements and their corresponding concentration in the clay sample.

Scanning Electron Microscopy and Electron Diffraction Spectrometry (SEM/EDS): VEGA 3 TESCAN type SEM (Model JSM 6510A) equipped with EDS (Figure 3.4) analyser was used for analysis of the coconut shell and the filter samples produced at different temperatures. The machine was operated at accelerating voltage of 15 kV. The samples were prepared using 2.5 glutaraldehyde for primary fixation followed by 1% Osmium tetroxide for secondary fixation to increase sample conductivity and minimize image distortions resulting from charging.

Transmission Electron Microscopy (TEM): A multipurpose TEM (JEM 2100F Model) was used to view samples of the coconut shell nanoparticle in order to obtain quantitative measurement and average particle size. The samples were prepared by drying on a copper grid with a thin film of carbon, followed by operation of the TEM with accelerating voltage of 100 keV with an AMT XR41-B 4-megapixel (2048 ×2048) bottom mount CCD camera was used to focus a beam of electron on the sample.

Brunauer-Emmett-Teller (BET): technique was used in determining the surface area of a material. The Dubinin – Radushkevich (D – R) method was used to calculate the surface area of the micropore. Then the surface area of the mesopore was calculated by subtracting the micropore surface area value from the BET surface area. To get the value of surface area for the BET, nitrogen was used at a temperature of 196 °C.

3.0 RESULTS AND DISCUSSION

3.1 Characterization of Clay and Coconut shell

3.1.1 X-Ray Fluorescence (XRF) of Clay

The XRF of clay sample showing its elemental composition is given in Table 2. This result indicates an alumino-silicate, clay type which falls under the illite clay mineral group. This result was further confirmed from the XRD results and is comparable to the results of Gaudette (1994). This clay type is preferred due to its weak shrinking and swelling ability causing it to maintain the product dimensions with change in temperature.

Table 2: XRF elemental analysis of clay sample

Elements	Si	Al	Ca	Mg	Mn	Fe	K	Cl	LOI
Composition (%)	65.30	15.70	1.50	0.94	0.02	7.67	0.29	0.07	8.51

3.1.2 X-Ray Diffraction of Clay

The result shown in Figure 6 revealed that the clay is characterized by two major peaks which are the Quartz (SiO₂) and the Aluminium Silicate (Al₂SiO₃) at diffraction angles (2θ) 26.9643° and 24.38° and interplanar distance of 3.31 and 3.65 respectively which confirmed the assertions made by the XRF result of a possible illite type clay (Gaudette, 1994). This describes the crystalline nature of the clay. Table 3 shows the distinctive list of identified phases.

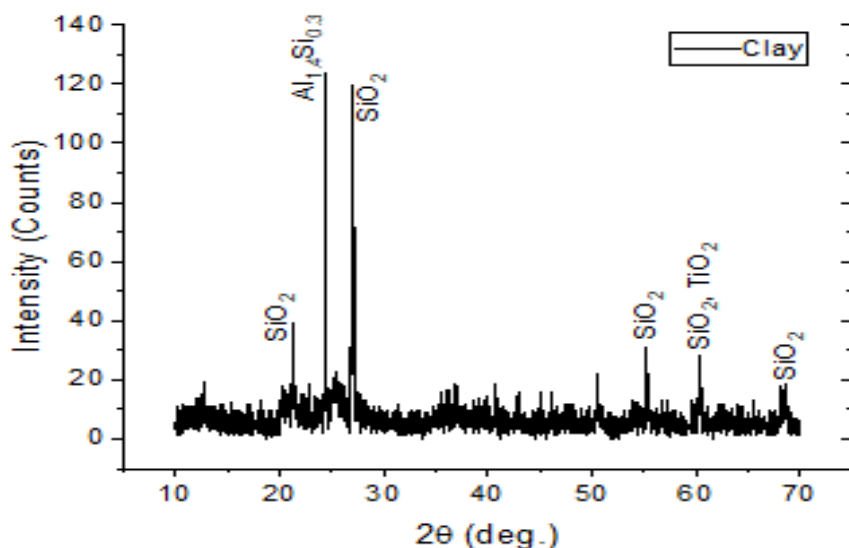


Figure 6: XRD profile of clay sample

Table 3: List of Identified phases for clay sample

Visible	Ref. Code	Score	Compound Name	Scale Factor	Chemical Formula
1	83-2470	50	Quartz, syn	0.537	Si O ₂
2	37-1461	20	Aluminum Silicate	1.000	Al _{1.4} Si _{0.3} O _{2.7}

2.1.3 SEM/EDS for coconut shell, carbonized coconut shell and activated carbon

The result of SEM/EDS analysis of coconut shell nanoparticle, carbonized coconut shell, and activated carbon from coconut shell is presented in Figures 7, 8 and 9. Figure 7 is the SEM/EDS morphology of coconut shell nanoparticles showed a rather shapeless, rough and uneven surface in the micrograph while the carbon content is 66.6 wt.% according to the corresponding EDS image. This type of surface is correspondent to the result obtained by Azrina *et al* (2021) for an uncarbonized and activated coconut shell particle. The result obtained from the EDS result is very close to the result of Ikumapayi and Akinlabi (2019) with about 65% carbon in the uncarbonized coconut shell.

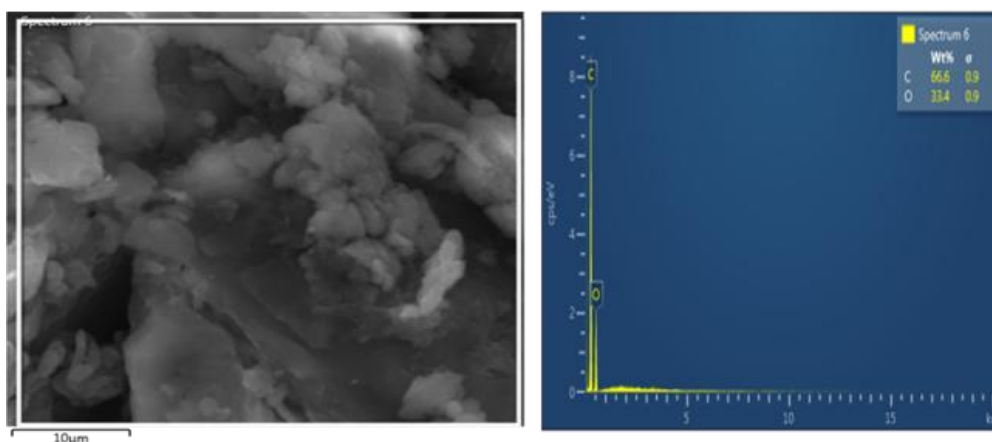


Figure 7: SEM/EDS of Coconut shell

Figure 8 shows result of the carbonized coconut shell with SEM giving a more defined structure but combined and the carbon content is 79.3 wt.%. The increase in carbon content displayed in the EDS image is an indication that carbonization was achieved at the temperature used (800°C).

This increase in carbon is comparable to the result obtained in the study of Bello *et al*, (2016) with an indicated carbon content of 78.68% after carbonization at 1000 °C. The microstructure showed a network kind of structure with more definite shape and presence of definite pores unlike the coconut shell nanoparticle in Figure 8 which is coherent with literatures (Gimba and Turoti, 2008; Bello *et al*, 2016; Yusop, *et al*, 2021).

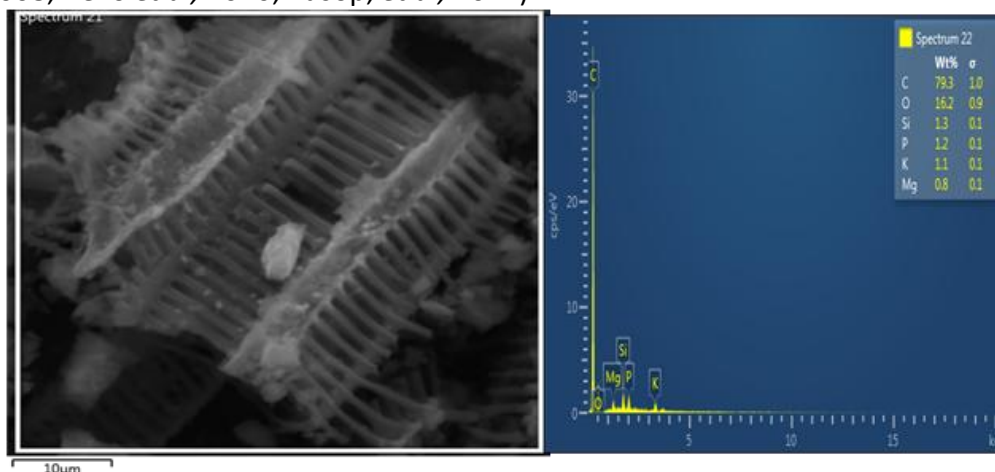


Figure 8: SEM/EDS analysis of CCS.

Figure 9 shows a particle and defined structure for activated carbon (AC) and the carbon content is 80.7 wt.%. The SEM image showed a more defined structure with pores or cavities distributed on the surface (Azrina, *et al*, 2021). These pores act as sites for adsorption which makes activated carbon good chemical molecules adsorbent (Azrina, *et al*, 2021; Yusop, *et al*, 2021). The pores created are as a result of the removal of moisture and other volatile matter from the coconut shell as a result of carbonization and activation causing the increased concentration of carbon in the structures as indicated by the EDS result.

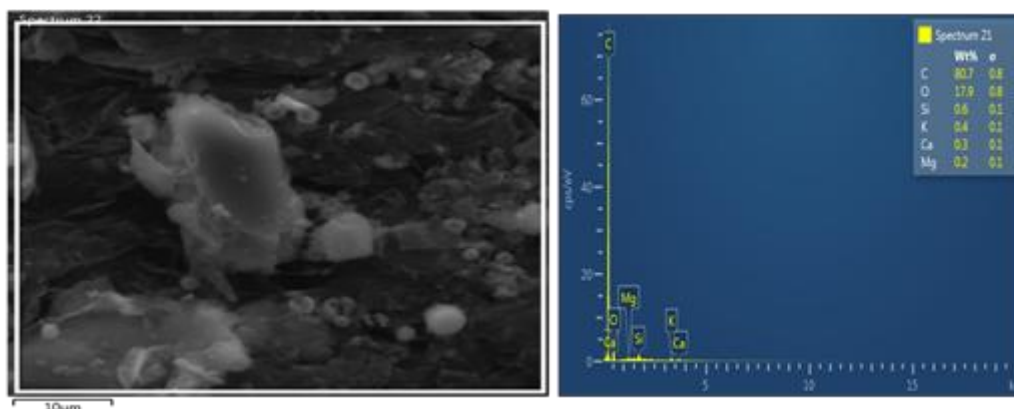


Figure 9: SEM/EDS morphology of AC

3.1.4 Transmission Electron Microscopy (TEM) of coconut shell nanoparticle

TEM analysis was carried out for coconut shell particle after 8 hours and 16 hours of milling the CS using ball mill. The result after 8 hours (Figure 13a) showed that the particles is not yet in nano scale while that at 16 hours (Figure 13b) showed that the material has nanoparticles. Particle size analysis on the TEM image summed up to an average particle size of 28.16 nm. The result of comparable with that obtained from the study of Kolawole *et al.*, (2016).

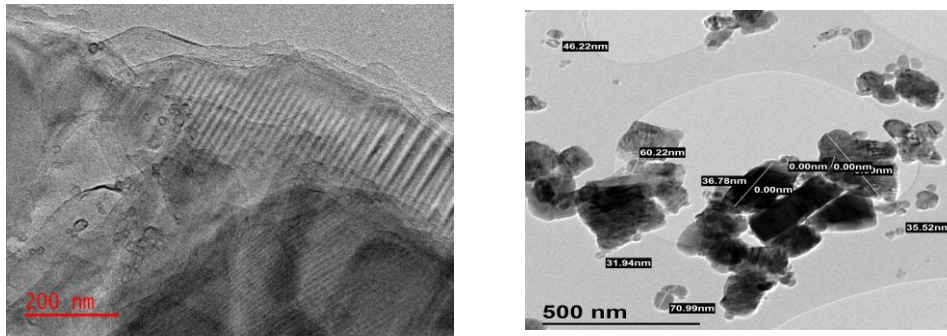


Figure 10 (a): TEM image after 8 hours of milling Figure 10 (b): TEM image after 16 hours of milling

3.2 Results from Firing of Clay Composite Filters

The firing of hybrid clay composite was carried out at temperature of 700 °C, 750 °C, 800 °C, 850 °C, 900 °C, 950 °C and 1000 °C.

At first, the firing was carried out at the rate of 150 °C per hour without prior gradual heating in the oven and the result was as produced in Figure 11. The study of Xiao *et al* (2021) studied how cracks are formed on the surface of red clay due to temperature change in the drying process at temperature of 23 °C, 40 °C and 60 °C. There is reduction in the time needed for crack initiation with increasing temperature making the crack rate faster while the cracks form all over the surface at almost the same time with different diameters when dried at 23 °C, 40 °C (Xiao *et al*, 2021). The first firing samples produced in this study were not acceptable and a slower drying and firing process was then set.



Figure 11: Result of firing at the rate of 150 °C per hour before oven drying

The drying for this second firing process was carried out at a temperature of 50 °C in the oven for 5 days with a record of steady reduction in size was achieved. When the weight range of the first firing samples were achieved which showed that the moisture is completely fried out, then the samples were ready for firing. The firing rate was also reduced to 75 °C/hr to the required temperature then left to cool in the furnace for 12 hours, then continued cooling in the open air. This process described above produced the samples in Figure 12 which are visibly not cracked. The change in color can firstly be attributed to heating at a temperature that is above 500 °C which according to Milheiro *et al* (2005) and Dong *et al* (2021) is as a result of the oxidation of the iron containing minerals in the clay to Fe³⁺. The cations of Fe³⁺ substitutes those of Al³⁺ at higher temperature causing the deeper red color and more reactions (Figure 12).



Figure 12: Filters produced from oven drying at 50 °C before firing at the rate of 75 °C/hr

3.3 X-Ray Diffraction (XRD) of Clay Composite Filter Samples

The XRD profiles of the filter samples fired at 800 °C, 900 °C and 1000 °C are given in Figures 13 to 15.

Figure 13 showed just one major peak in the sample fired at 800 °C, which is Quartz with the chemical formula SiO_2 at diffraction angle (2θ) of 27.21 and intensity of 52.81. Other visible peaks are Ertixiite, Quartz low, and Manganese Magnesium Oxide with chemical formula $\text{Na}_2\text{Si}_4\text{O}_9$, SiO_2 , and $(\text{MgO})_{0.59}(\text{MnO})_{0.41}$ at diffraction angle (2θ) 21.48, 50.68, and 60.66; and intensity of 16.73, 12.43, and 5.09 respectively. The wide gap between peaks indicates an amorphous solid material and comparing this figure with Figure 6, it can be seen that there is a reduction in the intensity of Silica and a disappearance of the Alumina phase from the peaks (Dong *et al*, 2021; Toledo *et al*, 2004). In the presence of organic matter like coconut shell carbonization takes place and so many other chemical changes occur. The equation of change in the carbon content is given below which is comparable to the study of Toledo *et al*, (2004). The equation 1 and 2 is also applicable to firing at 900 °C (Figure 14) and at 1000 °C (Figure 15) showing how the carbonaceous material (Coconut shell) is burned out of the filter samples.

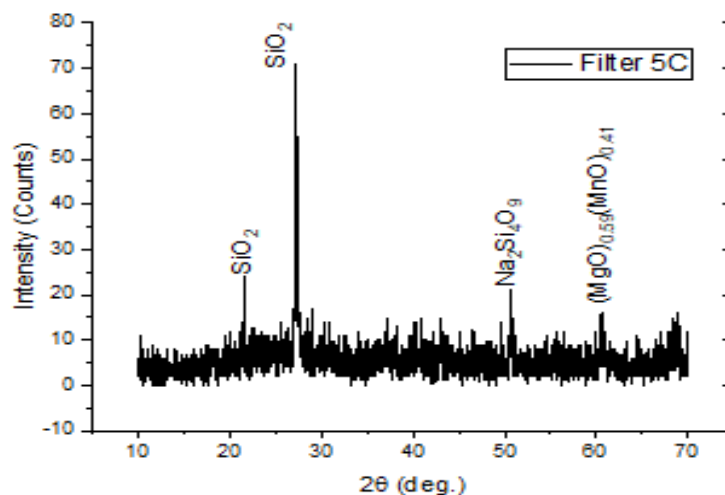


Figure 13: XRD of Filter sample fired at 800 °C

Table 4: List of Identified phases for filter sample fired at 800 °C

Visible	Ref. Code	Score	Compound Name	Displacement [°2Th.]	Scale Factor	Chemical Formula
1	83-2473	42	Quartz, syn	0.000	0.855	SiO ₂
2	39-0382	7	Ertixiite	0.000	0.121	Na ₂ Si ₄ O ₉
3	86-1563	6	Quartz low	0.000	0.086	SiO ₂
4	77-2379	6	Manganese Magnesium Oxide	0.000	0.285	(MgO) _{0.59} (MnO) _{0.41}

At firing temperature of 900 °C (Figure 14, Table 5), the result of XRD shows the presence of Silicon Oxide (SiO₂) in 2 peaks, another phase called periclase (MgO), sodium titanium oxide (Na₂TiO₃), and sodium calcium silicate (Na₂Ca[SiO₄]). The intensity of these peaks is 107.72 and 98.7, 79.06 and 21.77, 9.23, 98.70, and 6.27 respectively and their diffraction angles (2θ) are 27.30 and 40.09, 21.47 and 50.66, 43.04, 40.09, and 60.46. This sample has more identifiable peaks than that fired at 800 °C. There is possibility of increased reaction as a result of the increasing reduction environment created by the carbonaceous material (Toledo *et al*, 2004). The reaction that takes place from firing at 900 °C (Dong *et al*, 2021) is given in equation 3 and 4.

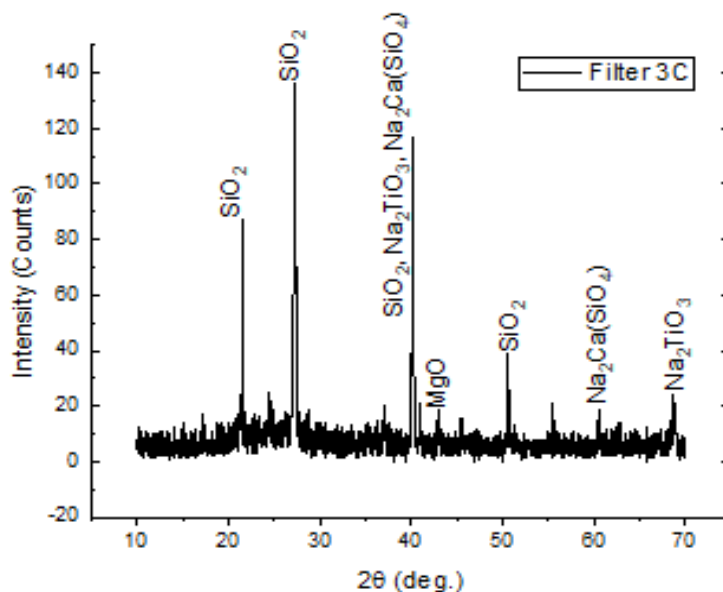


Figure 14: XRD of Filter sample fired at 900 °C

Table 5: List of Identified phases for Filter sample fired at 900 °C

Visible	Ref. Code	Score	Compound Name	Displacement [°2Th.]	Scale Factor	Chemical Formula
1	76-0931	42	Silicon Oxide	0.000	0.535	SiO ₂
2	81-0066	33	Silicon Oxide	0.000	0.761	SiO ₂
3	87-0653	22	Periclase	0.000	0.114	MgO
4	47-0130	21	Sodium Titanium Oxide	0.000	0.687	Na ₂ TiO ₃
5	02-0951	4	Sodium Calcium Silicate	0.000	0.168	Na ₂ Ca(SiO ₄)

Figure 15 and Table 6 shows the result of XRD of Filter sample fired at 1000 °C. This result displayed more peaks which is explained by the study of Dong *et al.*, (2021) as caused by the clay material when fired to 800 °C. The flux components of the clay start melting from 600 °C and a more stable material is gotten at temperature above 800 °C (Johari *et al.*, 2010).

Figure 15 has the highest peaks as silicon oxide (SiO₂) with intensity of 60.40 and diffraction angle (2θ) at 27.3. Followed by Quartz (SiO₂) with peaks of intensity, 60.40, 33.78, and 8.29 at diffraction angles (2θ) of 27.31, 37.15, and 21.47. Other identified phases are Magnesium Oxide (MgO₂), Corundum (Al₂O₃), Ertixiite (Na₂Si₄O₉), and Manganese Titanium Oxide (Mn₂TiO₄). Their intensities are 33.78, 16.56, 8.02 and 9.65 respectively with diffraction angles at (2θ) 37.15, 35.26, 50.78, and 60.23.

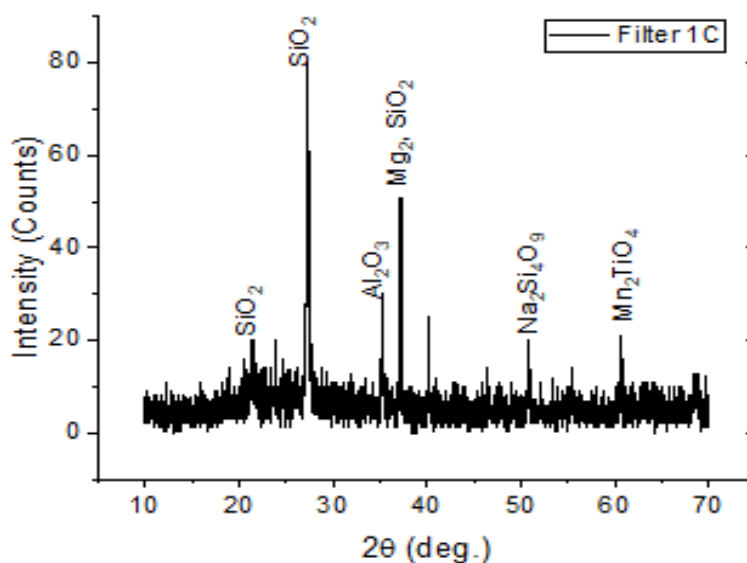


Figure 15: XRD of Filter sample fired at 1000 °C

Table 6: List of Identified phases for filter sample fired at 1000 °C

Visible	Ref. Code	Score	Compound Name	Displacement [°2Th.]	Scale Factor	Chemical Formula
1	81-0066	45	Silicon Oxide	0.000	0.745	SiO ₂
2	76-1363	20	Magnesium Oxide	0.000	0.639	MgO ₂
3	83-2472	25	Quartz, syn	0.000	0.273	SiO ₂
4	75-0784	12	Corundum	0.000	0.118	Al ₂ O ₃
5	39-0382	7	Ertixiite	0.000	0.023	Na ₂ Si ₄ O ₉
6	20-0728	5	Manganese Titanium Oxide	0.000	0.233	Mn ₂ TiO ₄

3.4 Scanning Electron Microscopy and Energy Dispersive X-ray spectroscopy of Clay Composite Filter samples

The SEM/EDS images obtained from sample filters fired at 800 °C, 900 °C, and 1000 °C is as shown in Figure 16 to 18. The EDS images has 3 peaks common to all the samples which are Silicon (Si), Aluminium (Al), and Oxygen (O) showing the Alumina (Al₂O₃) and Silica (SiO₂) which is the clay matrix elements as prevalent. Then the other elements present are Iron (Fe), Sodium (K), Titanium (Ti), Calcium (Ca), and Carbon (C). The present of some carbon still present in the 900 °C and 700 °C fired samples indicates the presence of some Activate carbon in the samples which will be an advantage to the adsorption property of the sample. The SEM image of the Filter samples shows the shapes of the phases present, pores, and how they are arranged. It is quite

difficult quantifying the pores using the SEM images which makes the BET result come handy with values of pore size and pore volume at different temperatures of firing. At 800 °C which the start of the organic material has just begin to carbonize creating spaces in the sample but not yet completely formed as shown in Figure 19. Sample fired at 900 °C showed finer distribution of the silicon oxide (SiO₂)

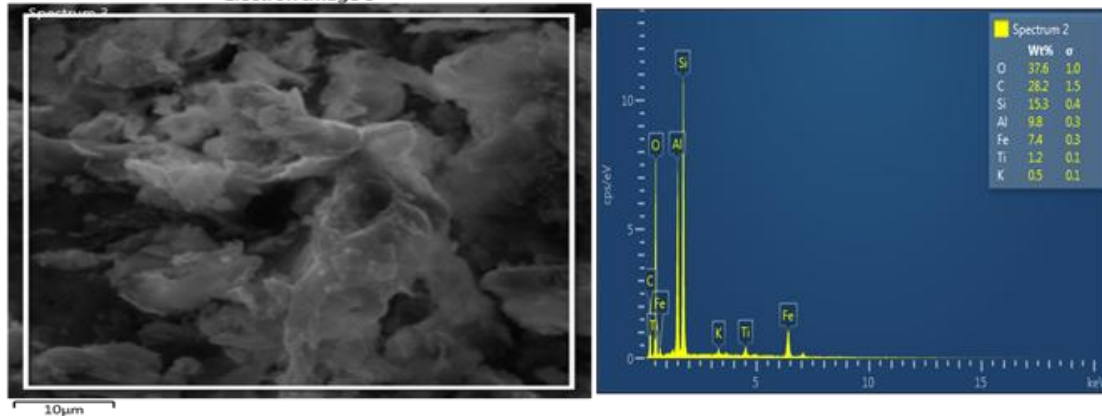


Figure 16: SEM/EDS profile of Filter sample fired at 800 °C

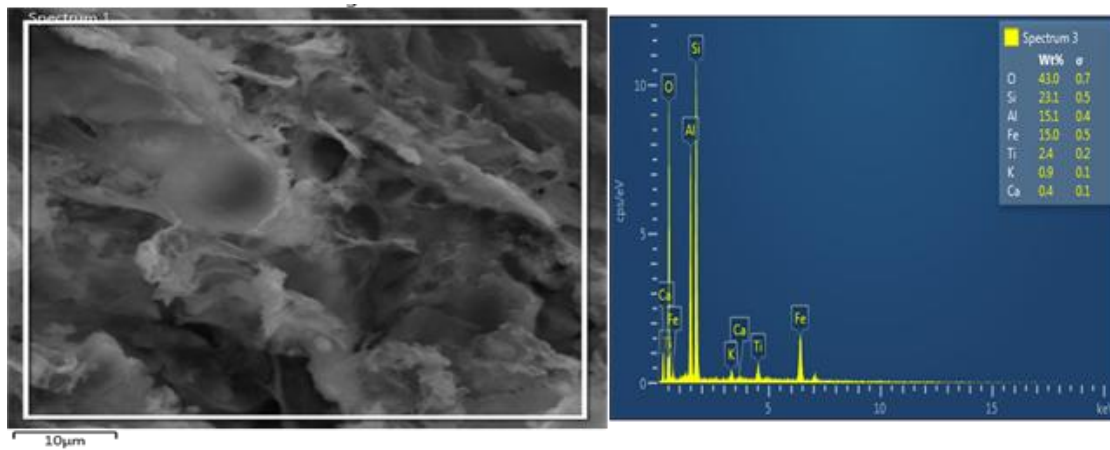


Figure 17 SEM/EDS of Filter sample fired at 900 °C

At 1000 °C firing, the sample SEM image showed a roughage when compared to the 900 °C fired sample which indicates less homogeneity in the structures and somewhat fusion in the material and this will cause reduction in the pore size of the material according to (Dura *et al*, 2019)

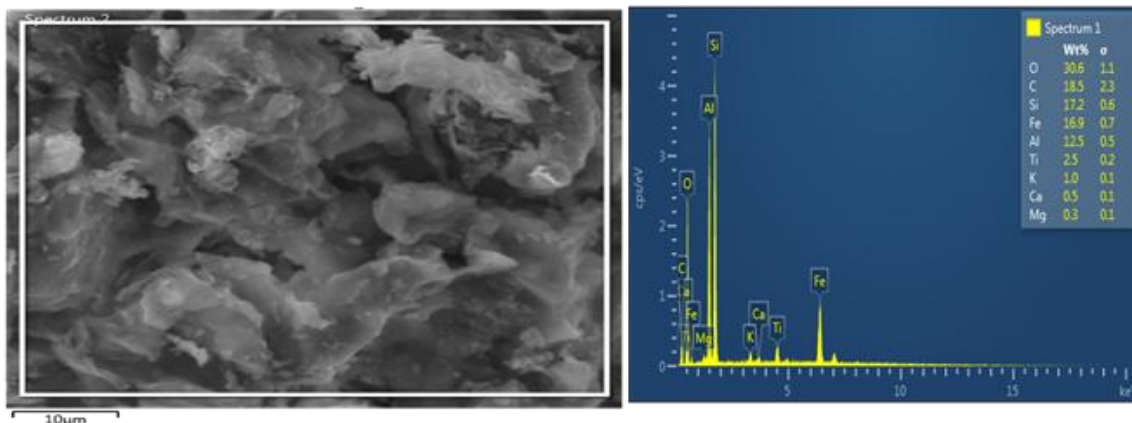


Figure 18: SEM/EDS of Filter sample fired at 1000 °C

3.5 BET of Composite Clay Filters

The pore size, pore volume, and surface area of filter samples of different blends fired at 700 °C, 800 °C, 900 °C, and 1000 °C were obtained from the results of the BET test and summarized in Table 7. The result showed that for sample with composition A, the pore size reduces with reducing firing temperature from 1000 °C up to 800 °C and then rapidly increased at 700 °C. At other compositions B, C, and D, there is higher value of pore size at 900 °C compared to other temperatures with a consistent increase obtained at 700 °C. This shows that there is a significant influence of temperature and composition on the filter samples. The result of increase in the pore size from 800 °C to 1000 °C firing temperature is consistent with the study of Hall *et al* (2012) and Dutra *et al* (2019).

Table 7: Physical properties of filters produced at different temperatures

Temperature S(°C)	Sample	Pore size (nm)	Pore Volume (m ³)	Surface Area (m ²)
1000	1A	8.04534	0.01930	6.0973
	1B	8.00002	0.00044	5.7110
	1C	8.52083	0.01099	11.0070
	1D	6.71202	0.04600	8.0050
900	3A	7.07502	0.02030	7.7890
	3B	8.06802	0.02134	8.1100
	3C	8.92483	0.02991	12.0020
	3D	6.81282	0.02600	8.0750
800	5A	7.06532	0.01630	6.7810
	5B	8.01812	0.01135	7.1000
	5C	8.90489	0.02999	11.5023
	5D	6.82288	0.01609	7.6750
700	7A	8.04530	0.01730	7.0900
	7B	8.01911	0.01225	6.1090
	7C	8.90343	0.02978	11.202
	7D	6.81188	0.01609	7.845

3.6 Flow Rate of Clay Composite Filters

The flow rate of the filter samples is as shown in Table 8. There is a significant increase in the flow rate with increasing temperature and increase in the wt.% of coconut shell nanoparticle. The effect of temperature and coconut shell is directly proportional to the flow rate of filter samples. The least flow rate was obtained from sample containing 10% coconut shell and 30% activated carbon while the highest flow rate was from samples with 30% coconut shell and 10% activated carbon. This increase in flowrate with increase in coconut shell content is due to an increase in the numbers of pores. These pores are created when the coconut shell present in the sample burns out as a result of firing. Peak values of flow rate were obtained for samples fired at 900 °C, therefore, this temperature can be set as the maximum required temperature for optimum flow rate. Further increase in firing temperature to 950 °C and 1000 °C led to a continuous reduction in the flow rate obtainable.

Table 8: Result of flow rate test carried out on the sample clay composite filters

Composition (Clay:AC:NPCS)	Flow Rate (L/hr)	Temperature (°C)						
		1000	950	900	850	800	750	700
A		2.14	2.24	2.25	1.46	1.41	0.05	0.17
B		2.20	2.43	2.41	2.75	1.89	0.23	0.26
C		2.21	2.48	2.77	2.93	2.02	0.30	0.30
D		2.37	2.67	2.92	2.48	2.63	0.37	0.35

4.0 CONCLUSION

This study produced a clay composite filter with different blends of clay, coconut shell nanoparticle and activated carbon at varying firing temperatures. The microstructural, and physical characteristics of developed filters were carried out and the efficiency of the filters was tested using BET method and the pore size with surface area of the different samples were compared to the final flow rate. Activated carbon was obtained from carbonized coconut shell using natural alkaline source like lemon and the use of ball mill for grinding of coconut shell produced a nanoparticle after 16 hours of grinding. The results obtained from the flow rate is corroborated by the BET result of pore size and pore volume of the filter samples where there is a steady increase in the pore size and pore volume from samples fired at 700 °C to 900 °C. The addition of activated carbon to the blend used for producing clay composite filters is not showing a significant change in the pore size, pore volume and flow rate.

ACKNOWLEDGEMENT

The authors recognize everyone who contributed to the successful completion of this research. Starting from Prof. Victor Aigbodion of UNN, Nsukka to Engr. Sulaimon, Engr. Pogoson, Engr. Kola and Engr. Isaac of UNILAG, Department of Metallurgical and Materials Engineering Laboratory.

REFERENCES

- Azrina, A., Khan, M., Yusop, M., Jaya, E., Jaya, M. and Azmier, M. (2021). Single-Stage Microwave-Assisted Coconut-Shell-Based Activated Carbon for Removal of Dichlorodiphenyltrichloroethane (DDT) from Aqueous Solution: Optimization and Batch Studies. *International Journal of Chemical Engineering*, 1-15. <https://doi.org/10.1155/2021/9331386>.
- Babangida, A., Aslanova, D., Elkiran, G., 2022. A research on relationship of environment and effect of water diseases in Nigeria. *Journal Of Optoelectronics Laser*, 41 (12): 267–273
- Bello, S. A., Agunsoye J. O., Adebisi J. A., Kolawole F. O. and Hassan S. B. (2016). Physical Properties of Coconut Shell Nanoparticles. Kathmandu University; *Journal of Science. Engineering and Technology*, 12 (1): 63-79
- Berg, P. A. (2015) The world's need for household water treatment, *Journal of American Water Works Association*, 107 (10): 36-44
- Dong, Z., Sun, Q. and Zhang, W. (2021). Physical and Mechanical Properties of Clay After Heating in Different Oxygen Levels and Cooling with Different Methods. *Research Square*. <https://doi.org/10.21203/rs.3.rs-501548/v1>
- Dutra, L., Freitas, M., Grillet, A.-C., Mendes, N. and Woloszyn, M. (2019). Microstructural Characterization of Porous Clay-Based Ceramic Composites. *Materials*, 12: 946. <https://doi.org/10.3390/ma12060946>
- Erhuanga, E., Banda, M.M., Kiakubu, D., Kashim, I.B., Ogunjobi, B., Jurji, Z., Ayoola, I. and Soboyejo, W. (2021). Potential of ceramic and biosand water filters as low-cost point-of-use water treatment options for household use in Nigeria. *Journal of Water, Sanitation and Hygiene for Development*, 11 (1): 126-140
- Farrow, C., McBean, E, Huang, G., Yang, A. L., Wu, Y. C., Liu, Z., Dai, Z. N., Fu, H. Y., Cawtel, T. and Li, Y.P. (2018). Ceramic Water Filters: A Point-of-Use Water Treatment Technology to remove Bacteria from Drinking Water in Longhai City, Fujian Province, China. *Journal of Environmental Informatics*, 32 (2): 63-68
- Gaudette, H. E. (1964). The Nature of Illite. *Clays and Clay Minerals*, 13 (1): 33–48
- Gimba, C. E. and Turoti, M. (2008). Optimum Condition for Carbonisation of Coconut shells. *Scientia Africana*, 7 (4): 12-21
- Hall, M., Tsang, S., Casey, S., Khan, M. and Yang, H. (2012). Synthesis, characterization and hygrothermal behaviour of mesoporous silica high-performance desiccants for relative humidity buffering in closed environments. *Acta Mater.* 60: 89–101
- Ikumapayi, O.M. and Akinlabi, E.T. (2019). Image Processing and Particle Size Analysis of Coconut Shell Nanoparticles. *International Journal of Civil Engineering and Technology (IJCIET)*. 10 (2): 2475–2482
- Johari, I., Said, S., Abu, B., Bakar, B. H. and Ahmad, Z. (2010). Effect of the change of firing temperature on microstructure and physical properties of clay bricks from Beruas (Malaysia). *Science of Sintering*, 42 (2)
- Kallman, E. N., Oyanedel-Craver, V. A. and Smith, J. A. (2011). Ceramic Filters Impregnated with Silver Nanoparticles for Point-of-Use Water Treatment in Rural Guatemala. *Journal of Environmental Engineering*, 137 (6): 407-415

- Kolawole, F.O., Agunsoye, J. O., Bello, S. A., Adebisi, J. A., Okoye, O. C. and Hassan, S. B. (2016). Particle Size Analysis and Characterization of Cassava (*Manihot esculenta crantz*) Stem Nanoparticles (CSNPs) via a Top-down Approach. *Annals of Science and Technology B*, 1 (1): 52-55
- Mellor, J. E., Kallman, E., Oyanedel-Craver, V. and Smith, J. A. (2014). Comparison of Three Household Water Treatment Technologies in San Mateo Ixtatan, Guatemala. *Journal of Environmental Engineering*
- Milheiro, F. A. C., Freire, M. N., Silva, A. G. P. and Holanda, J. N. F. (2005). Densification Behaviour of a red firing Brazilian Kaolinite clay. *Ceramic International*, 31: 757-763
- Murphy, H., Sampson, M., McBean, E. and Farabakhsh, (2010a). Influence of household practices on the performance of clay pot water filters in rural Cambodia. *Desalination*. 252: 145-152
- Murphy, H., McBean, E. and Farabakhsh. (2010b). Microbial and chemical assessment of ceramic and biosand water filters in rural Cambodia. *Water Science and Technology Water Supply*, 10: 286.-295
- Murphy, H., McBean, E. and Farabakhsh, (2010c) A critical evaluation of two point-of-use water treatment technologies: Can they provide water that meets WHO drinking water guidelines? *Journal of Water and Health*, 8: 611-630
- National Research Council (1999). Identifying Future Drinking Water Contaminants Washington, DC The National Academies Press
- NBS UNICEF (2017). Multiple Indicator Cluster Survey 2016– 17, Survey Findings Report. National Bureau of Statistics and United Nations Children’s Fund, Abuja, Nigeria.
- Pagsuyoin, S. A., Santos, J. R., Latayan, J. S. and Barajas, J. R. (2015). A multi-attribute decision making approach to the selection of point-of-use water treatment. *Environment Systems and Decisions*. 35 (4): 437–452.
- Perez-Vidal, A., Diaz-Gomez, J., Castellanos-Rozo, J. and Usaquen-Perilla, O. G. (2016). Long-term evaluation of the performance of four point-of-use water filters. *Water Resources*, 98: 176-182.
- Santos, J., Pagsuyoin, S. A. and Latayan, J. (2016). A multi-criteria decision analysis framework for evaluating point-of-use water treatment technologies. *Clean Technologies and Environmental Policy*, 18 (5): 1263–1279.
- Saputro, E. A., Wulan, V. D. R., Winata, B. Y., Yogaswara, R. R. and Erliyanti, N. K. (2020). The process of activated carbon from coconut shells through chemical activation. *Journal of Science and Technology*, 9 (1): 23-28.
- Toledo, R., dos Santos, D. R., Faria, R. T., Carrio, J. G., Auler, L. T. and Vargas, H. (2004). Gas release during clay firing and evolution of ceramic properties. *Applications of Clay Science*, 27: 151–157
- UNICEF 2023. Goal 6: clean water and sanitation, Ensure availability and sustainable management of water and sanitation for all. UNICEF Data. <https://data.unicef.org/sdgs/goal-6-clean-water-sanitation/>, Accessed 22/01/2023
- United Nations (UN) (2023): Goal 6: Ensure access to water and sanitation for all. UN Regional Information Center for Western Europe: <https://unric.org/en/sdg-6/>, Accessed 21/12/2023
- WHO, African Region 2021. Water. WHO Regional Office for Africa: <https://www.afro.who.int/health-topics/water>, Accessed 22/01/ 2023
- WHO/UNICEF (2021): Progress on household drinking water, sanitation and hygiene 2000 – 2020 Five years into the SDGs. Drinking Water UNICEF Data. Geneva: World Health Organization (WHO) and the United Nations Children’s Fund (UNICEF): <https://www.unwater.org/sites/default/files/app/uploads/2021/07/jmp-2021-wash-households-LAUNCH-VERSION.pdf>, Accessed 20/05/2022
- World Health Organization/ UNICEF (2014): Progress on drinking water and sanitation: 2014 update WHO; UNICEF
- Xiao, G., Ye, Z., Xu, G., Zeng, J. and Zhang, L. (2021). Temperature Effect on Crack Evolution of Red Clay in Guilin. *Water*, 13 (21): 3025.
- Yusop, M. F. M., Ahmad, M. A., Rosli, N. A., Gonawan, F. N., and Abdullah, S. J., (2021). Scavenging malachite green dye from aqueous solution using durian peel based activated carbon. *Malaysian Journal of Fundamental and Applied Sciences*, 17: 95–103